Monthly Notices
of the
ROYAL ASTRONOMICAL SOCIETY

MNRAS **433,** 1015–1022 (2013) doi:10.1093/mnras/stt782
Advance Access publication 2013 June 3

AGN in dusty hosts: implications for galaxy evolution

M. Symeonidis,[1]⋆ J. Kartaltepe,[2] M. Salvato,[3] A. Bongiorno,[4] M. Brusa,[3] M. J. Page,[1] O. Ilbert,[5] D. Sanders[6] and A. van der Wel[7]

[1]*Mullard Space Science Laboratory, University College London, Holmbury St Mary, Dorking, Surrey RH5 6NT, UK*
[2]*National Optical Astronomy Observatory, 950 N. Cherry Ave, Tucson, AZ 85719, USA*
[3]*Max-Planck-Institut fur extraterrestrische Physik, Giessenbachstrasse 1, D-85748 Garching, Germany*
[4]*INAF – Osservatorio Astronomico di Roma, via di Franscati 33, I-00040 Monte Porzio Catone, Italy*
[5]*Laboratoire d'Astrophysique de Marseille, Universite de Provence, CNRS, BP 8, Traverse du Siphon, F-13376 Marseille Cedex 12, France*
[6]*Institute for Astronomy, 2680 Woodlawn Drive, University of Hawaii, Honolulu, HI 96822, USA*
[7]*Max-Planck-Institute for Astronomy, Koenigstuhl 17, D-69117 Heidelberg, Germany*

Accepted 2013 May 3. Received 2013 April 21; in original form 2012 September 14

ABSTRACT

We present strong empirical evidence for a physical connection between the occurrence of a starburst (SB) and a luminous active galactic nucleus (AGN) phase. Drawing infrared (IR), X-ray and optically selected samples from COSMOS, we find that the locus of type II AGN hosts in the optical colour–magnitude ($U - V/V$) and colour–colour ($U - V/V - J$) space significantly overlaps with that of IR-luminous ($L_{\rm IR} > 10^{10}$ L$_\odot$) galaxies. Based on our observations, we propose that, when simultaneously building their black hole and stellar masses, type II AGN hosts are located in the same part of colour–colour space as dusty star-forming galaxies. In fact, our results show that IR-luminous galaxies at $z < 1.5$ are on average three times more likely to host a type II AGN ($L_{\rm X} > 10^{42}$ erg s^{-1}) than would be expected serendipitously, if AGN and star-formation events were unrelated. In addition, the optical and IR properties of the AGN/SB hybrid systems tentatively suggest that the AGN phase might be coeval with a particularly active phase in a galaxy's star-formation history. Interestingly, we also find a significant fraction of type II AGN hosts offset from the dusty galaxy sequence in colour–colour space, possibly representing a transitional or post-SB phase in galaxy evolution. Our findings are consistent with a scenario whereby AGN play a role in the termination of star formation in massive galaxies.

Key words: galaxies: active – galaxies: evolution – galaxies: starburst – infrared: galaxies – X-rays: galaxies.

1 INTRODUCTION

It has long been proposed that black hole growth and starburst (SB) activity follow connected evolutionary paths, inter-regulated through complex feedback processes and eventually resulting in the observed black hole – bulge relationship (e.g. Magorrian et al. 1998; Silk & Rees 1998). In the context of extragalactic studies, a popular tool for studying galaxy evolution is the rest-frame optical colour–magnitude diagram (CMD) where the position of each galaxy in colour–magnitude space is linked to its evolutionary state (e.g. Strateva et al. 2001; Baldry et al. 2004; Weiner et al. 2005). The CMD appears bimodal, where most late types lie in the blue cloud and most early-type galaxies in the red sequence, with the region between the two (the 'green valley'; e.g. Wyder et al. 2007) being sparsely populated. The latter observation has led to the conclusion that galaxies spend only a small fraction of their lifetime in transit from the blue cloud to the red sequence, which has in turn founded speculations that energetic events associated with the central accreting black hole (active galactic nucleus, AGN) could be responsible for terminating star formation on short time-scales (e.g. Granato et al. 2004; Springel, Di Matteo & Hernquist 2005). As a result, the search for evidence of AGN feedback in extragalactic surveys has been to a large extent pursued through examination of the properties of green galaxies and type II AGN hosts. However, these studies have not always been in agreement with respect to whether green galaxies are a transition population or whether the colours of type II AGN hosts are an indication of the quenching of star formation (e.g. Martin et al. 2007; Westoby, Mundell & Baldry 2007; Georgakakis et al. 2008; Brammer et al. 2009; Brusa et al. 2009; Schawinski et al. 2009; Cardamone et al. 2010).

Here we aim to address the topic of SB/AGN synergy, using a sample of X-ray-selected type II AGN and a sample of 70 μm-selected galaxies from the COSMOS 2 deg^2 field. Previous work on 70 μm populations (Symeonidis et al. 2008, 2009, 2010; Kartaltepe et al. 2010a,b) has shown that the selection at 70 μm

⋆ E-mail: m.symeonidis@ucl.ac.uk

enables the assembly of a homogeneous sample of infrared (IR) luminous ($L_{\rm IR} > 10^{10}$ L$_\odot$) sources, characterized by large star-formation rates (SFRs). The motivation for this work is to investigate the link (if any) between black hole accretion and star formation, by comparing the location of AGN hosts in the colour–magnitude ($U - V$ versus M_V) and colour–colour ($U - V$ versus $V - J$) diagrams (e.g. Nandra et al. 2007; Rovilos & Georgantopoulos 2007; Hickox et al. 2009; Silverman et al. 2009; Treister et al. 2009; Bongiorno et al. 2012) to that of IR-luminous galaxies (Kartaltepe et al. 2010b; Symeonidis et al. 2010).

The paper is laid out as follows: in Section 2 we describe the sample and in Section 3 we present our results and analysis. Our conclusions are reported in Section 4. Throughout, we adopt a concordance cosmology of $H_0 = 70$ km s^{-1} Mpc^{-1}, $\Omega_{\rm M} = 1 - \Omega_\Lambda = 0.3$.

2 OBSERVATIONS

2.1 The data

Our data come from the 2 deg^2 COSMOS field (Scoville et al. 2007). The optical sample consists of 438 226 objects with $i^+_{\rm auto}$ (Subaru) $<$ 25 (AB), with 30-band imaging data combined for the derivation of photometric redshifts and rest-frame magnitudes (see Capak et al. 2007; Ilbert et al. 2009). In this work we also take advantage of the 24 and 70 μm *Spitzer*/MIPS observations (Frayer et al. 2009; Le Floc'h et al. 2009) acquired as part of the *Spitzer* COSMOS legacy survey (Sanders et al. 2007), as well as the ∼50 ks *XMM–Newton* survey of the COSMOS field (Cappelluti et al. 2007, 2009; Hasinger et al. 2007). The 70 μm catalogue used in this work together with details on the multiwavelength data cross-matching and in-depth analysis of the 70 μm population is presented in Kartaltepe et al. (2010a,b). The *XMM–Newton* X-ray catalogue is compiled and cross-matched to the optical sample in Brusa et al. (2010). There are 1550 extragalactic X-ray sources with unambiguous optical counterparts.

2.2 The sample

We exclude 26 per cent of the optical sample, as they have a flag which indicates that they are near a bright source, such as a star, and so their photometry might be contaminated. We also exclude from subsequent analysis the <6 per cent of sources which do not have available redshifts. Finally, we cut the three data sets (optical, IR and X-ray) down to the same coverage area, leaving us with 304 627 sources in the optically selected sample. Out of those, 1274 are detected at 70 μm with $f_{70} > 7.5$ mJy ($>5\sigma$), hereafter the IR galaxy sample, and 1394 have $L_{\rm X} > 10^{42}$ erg s^{-1} in either the soft or the hard band, which we take to be our AGN sample. Note that the optical rest-frame magnitudes for the X-ray AGN come from Salvato et al. (2009) and for all other sources from Ilbert et al. (2009).

About half of the AGN have spectroscopic redshifts and the remaining have good quality photometric redshifts from Salvato et al. (2009, 2011). 27 per cent of the AGN are spectroscopically classified as broad line (BLAGN; line full width at half-maximum > 2000 km s^{-1}; Brusa et al. 2010). For the work presented here, we remove BLAGN, because the galaxy photometry is significantly contaminated by the active nucleus. We also exclude AGN which do not have spectroscopic redshifts, but which are classified as type I through spectral energy distribution (SED) fitting to the optical photometry (see Salvato et al. 2009; Bongiorno et al. 2012). This leaves a total of 856 AGN hosts. Hereafter, when referring to AGN, it is implied that these are all type II and hence the optical photometry is dominated by the host galaxy.

The rest-frame colour–magnitude ($U - V$ versus M_V) and colour–colour ($U - V$ versus $V - J$) distributions of X-ray AGN hosts and the IR galaxy sample are shown in Fig. 1, overlaid on the optically selected COSMOS population. The COSMOS sample shows a peak at blue colours ($U - V \sim 0.5$; the 'blue cloud') and a peak at red colours ($U - V \sim 1.3$; the 'red sequence'). The transition region between the two peaks, at green ($U - V \sim 1$–1.2) colours, is more sparsely populated, the so-called green valley (see also Kartaltepe et al. 2010b). We observe a remarkable overlap between the AGN hosts and IR galaxies as they span the same range in the $U - V$ colour and cluster at the high V-band luminosity end occupied by massive galaxies. The colours of the IR sample are a consequence of dust reddening rather than age-related reddening, more evident in colour–colour space where age-reddened galaxies are offset from the sequence of IR galaxies (the 'dusty galaxy sequence'), towards bluer $V - J$ colours; see also Kartaltepe et al. (2010b), Wuyts et al. (2009), Williams et al. (2009) and Whitaker et al. (2011). Particularly noteworthy is that AGN hosts lie in two camps in colour–colour space: some have colours consistent with the dusty sequence of star-forming galaxies (SFGs), whereas a large fraction have bluer $V - J$ colours, offset from the dusty galaxy sequence. These characteristics are examined in detail in Section 3.

Out of the 856 type II AGN hosts in our sample, 66 are also 70 μm detected. In order to ensure that for these sources the 70 μm emission is host galaxy dominated, i.e. linked to star formation, the 70 μm to 24 μm flux density ratio is used as a discriminator between AGN- and star-formation-dominated far-IR emission, as described in Mullaney et al. (2010). Note that this criterion can be considered reliable up to $z \sim 1.5$; hence, we restrict all subsequent analysis to the $0.1 < z < 1.5$ redshift range, where the lower redshift cut serves to remove local, extended sources. AGN with $f_{70}/f_{24} > 6$ are taken to be host galaxy dominated in the IR – 45 sources in total at $0.1 < z < 1.5$, hereafter referred to as the AGN/SB hybrids. In addition, we restrict the IR galaxy sample to sources with $f_{70}/f_{24} > 6$ in order to exclude any sources which potentially host an AGN not detected in the X-rays but dominant in the mid/far-IR. Our final sample consists of 208 512 optically selected sources at $0.1 < z < 1.5$, of which 1156 are IR emitters, 634 host AGN and 45 are AGN/SB hybrids.

Hereafter, we use the terms 'IR galaxies', 'SFGs' and 'SBs' interchangeably throughout this paper and 'IR emission' refers to infrared emission from the host galaxy linked to star formation.

2.3 Sample properties

Fig. 2 shows the X-ray versus total IR luminosity of the 45 hybrid sources, against the X-ray–IR correlations for SFGs taken from Symeonidis et al. (2011b) for $L_{\rm IR} > 10^{11}$ L$_\odot$ sources (luminous and ultraluminous infrared galaxies, LIRGs and ULIRGs). To calculate X-ray luminosities, the soft and hard fluxes are K-corrected using a photon index $\Gamma = 1.9$, whereas the total IR luminosities are taken from Kartaltepe et al. (2010a). We note that the X-ray luminosities of the hybrid sources are offset by at least 2σ from the mean star-formation relations in the hard and soft X-ray bands. At lower IR luminosities ($L_{\rm IR} < 10^{11}$ L$_\odot$) there is some evidence that these relations might have a flatter slope (e.g. Lehmer et al. 2010); nevertheless, the $L_{\rm IR} < 10^{11}$ L$_\odot$ hybrids in our sample would still remain well above them. As a result, X-ray emission from all AGN/SB hybrids can be considered entirely AGN dominated. In fact, in

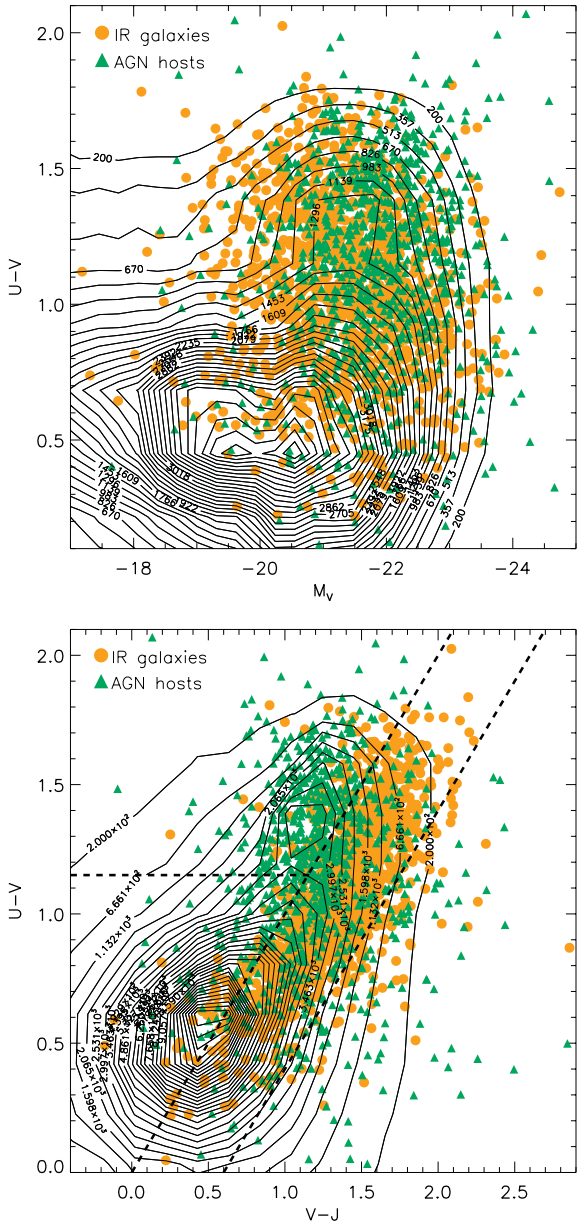

Figure 1. Top panel: the rest-frame $U-V$ versus M_V distribution for the IR galaxy sample (orange circles) and AGN hosts (green triangles). The contours represent the number of optically selected COSMOS sources in bins of 0.3 mag in M_V and 0.2 mag in $U-V$. There are 30 contours drawn in equal steps starting at 200 and ending at 4740 sources. The 'green valley' is around $U-V\sim1.1$ (see also Kartaltepe et al. 2010b). Lower panel: the rest-frame $U-V$ versus $V-J$ distribution for the IR galaxy sample (orange circles) and AGN hosts (green triangles). The contours represent the number of optically selected COSMOS sources in bins of 0.2 mag in both axes. There are 30 contours drawn in equal steps starting at 200 and ending at 13 717 sources. The dashed lines roughly outline the region traditionally occupied by age-reddened galaxies (top-left quadrant) and region of parameter space occupied by the IR galaxy sample, the 'dusty galaxy sequence' (parallel lines).

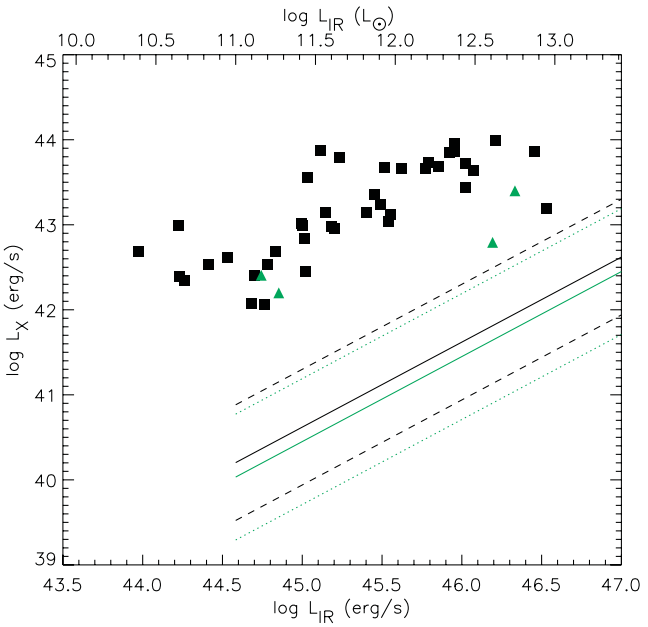

Figure 2. X-ray versus total IR luminosity of the 45 AGN/SB hybrids in our final sample. When a source does not have a hard band detection (shown as a black square), then we plot its soft X-ray luminosity (shown as a green triangle). The solid lines denote the X-ray/IR correlations for $L_{\rm IR}>10^{11}\,{\rm L}_{\odot}$ galaxies (LIRGs and ULIRGs) which are star-formation dominated in both the X-rays and the IR (taken from Symeonidis et al. 2011b). The black solid and dashed lines denote the *hard* X-ray–IR correlation ($\log L_{\rm HX}=\log L_{\rm IR}-4.38$) and $\pm2\sigma$ boundaries (±0.68 dex). The green solid and dotted lines denote the *soft* X-ray–IR correlation ($\log L_{\rm SX}=\log L_{\rm IR}-4.55$) and $\pm2\sigma$ boundaries (±0.74 dex). Note that the AGN/SB hybrids are offset from the relations for SFGs by at least 2σ, indicating that their X-ray emission can be assumed to be entirely AGN dominated. On the other hand, their IR emission is star-formation dominated (see the main text).

Symeonidis et al. (2010) we showed that a 200 ks X-ray survey is largely insensitive to X-ray emission from star formation, and in the hard band even a 2 Ms survey is insensitive to X-ray emission from star formation (Symeonidis et al. 2011b), suggesting that our AGN sample is not contaminated by sources where star formation substantially contributes or dominates the X-ray emission.

Fig. 3 shows the absolute V-band magnitude as a function of redshift in the redshift range of interest ($0.1<z<1.5$), for the optically selected sample, the AGN hosts and IR galaxies. The AGN hosts and IR galaxies are more optically luminous than the average optically selected galaxy at each redshift, suggesting that they are also more massive as optical luminosity correlates with stellar mass (e.g. Shapley et al. 2001, Savaglio et al. 2005). Fig. 4 shows the redshift distribution of the three galaxy types. We note that the AGN hosts peak at higher redshift than the IR galaxies, whereas the general population of optically selected galaxies have a relatively flat distribution. Restricting the latter to the brightest sources with $M_V<-20$, which is the range in M_V probed by the AGN and IR galaxies (see Fig. 3), we find that the redshift distribution of the optical sample now peaks at higher redshifts, similar to the AGN hosts.

3 RESULTS AND ANALYSIS

3.1 The distribution of AGN and IR galaxies in colour–magnitude and colour–colour space

In Figs 5 and 6, we show the colour–magnitude and colour–colour distributions for the AGN hosts and IR galaxies. They are binned and

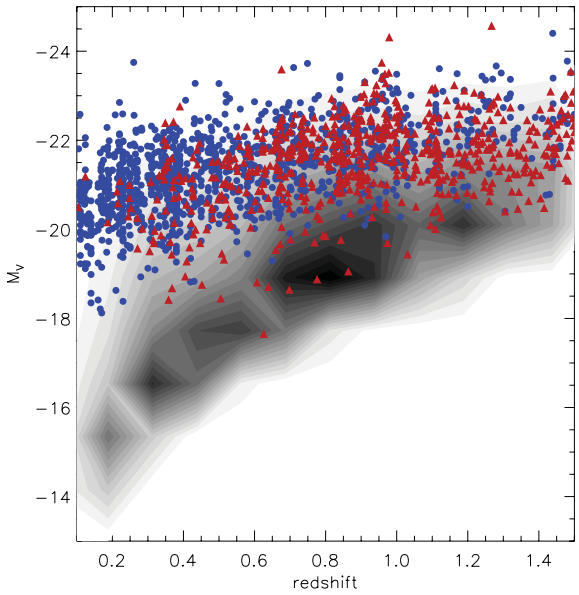

Figure 3. *V*-band absolute magnitude versus redshift for the samples used in this work – the optical population (grey filled-in contours), the AGN hosts (red triangles) and the IR galaxies (blue circles).

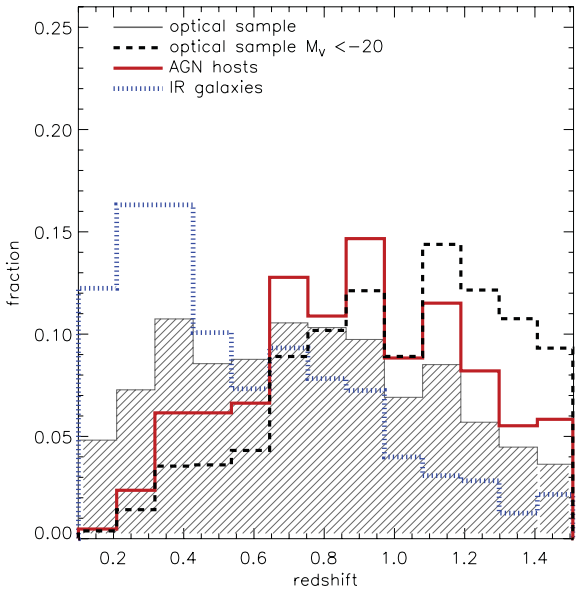

Figure 4. The redshift distributions of the samples used in this work. Each histogram is normalized to the total number of sources in the corresponding sample. Note that although the underlying optically selected population has a relatively flat distribution, restricting it to the most optically bright sources ($M_V > -20$) skews it towards higher redshifts.

displayed as contours and further split into two redshift bins ($0.1 < z < 0.8$ and $0.8 < z < 1.5$). The overlap noted in Fig. 1 is now seen more clearly; however, differences between the two populations also begin to emerge. We note that the peaks of the two distributions are well aligned in M_V but not in $U - V$, with AGN hosts peaking at redder colours. Moreover, many AGN hosts show bluer $V - J$ and redder $U - V$ colours consistent with those of red-sequence galaxies, offset to the left of the dusty galaxy sequence. These observations give weight to the notion that AGN host galaxies are not a uniform population. They also suggest that some AGN hosts have colours indicative of star formation and dust extinction, whereas others have colours consistent with an overall slowing down or termination of star formation.

3.2 The incidence of AGN hosted by IR galaxies

The high incidence of AGN and IR galaxies in similar parts of colour–magnitude and colour–colour space raises an important question: 'Is it simply a coincidence?' To address this point, we start by examining what we would expect if the answer were 'yes' and make the following probability argument: If AGN incidence and IR emission were independent, unrelated events in a galaxy of a given location in colour–magnitude or colour–colour space, what characteristics should the distributions of those hybrid AGN/SB sources have? To answer this question, we compute the expected number ($N_{\rm exp}$) and distribution of hybrid AGN/SB sources, under the assumption that IR emission and AGN incidence in a given galaxy are independent events. We take binned colour–magnitude (bin size of 0.5 in M_V and 0.25 in $U - V$; Fig. 5, top panel) and colour–colour distributions (bin size of 0.25 in $V - J$ and 0.25 in $U - V$; Fig. 6, top panel), allowing us to probe sources with similar optical properties (in each bin). For each bin, we count the number of optically selected sources, IR galaxies and AGN hosts and calculate the probability that an optically selected source is both star forming and hosts an AGN:

$$\frac{n_{i,\rm AGN}}{n_{i,\rm opt}} \times \frac{n_{i,\rm IR}}{n_{i,\rm opt}} = P_i(\rm AGN) \times P_i(\rm IR) = P_i(\rm AGN \cap IR), \quad (1)$$

where $n_{i,\rm opt}$, $n_{i,\rm AGN}$ and $n_{i,\rm IR}$ are the number of optically selected galaxies, AGN and IR-selected galaxies, respectively, in a colour–magnitude or colour–colour bin i, and P_i(AGN) is the probability that a galaxy hosts an AGN, whereas P_i(IR) is the probability that a galaxy is IR luminous and hence intensely star forming. Subsequently, we compute the expected number of galaxies in bin i, which are both IR luminous and host an AGN:

$$N_{i,\rm exp} = P_i(\rm AGN \cap IR) \times n_{i,\rm opt}. \quad (2)$$

Finally, the total number of expected hybrids $N_{\rm exp}$ is calculated by summing over all bins, i.e.

$$N_{\rm exp} = \sum_i N_{i,\rm exp}. \quad (3)$$

For each bin, the error on the expected number, $N_{i,\rm exp}$, is calculated by computing binomial errors on P_i(AGN) and P_i(IR) at the 68 per cent confidence interval ($\sim 1\sigma$) and assuming no error on $n_{i,\rm opt}$. The errors on $N_{i,\rm exp}$ from all bins are then added in quadrature to estimate the uncertainty on $N_{\rm exp}$. The expected colour–magnitude and colour–colour distributions (i.e. $N_{i,\rm exp}$) are shown in Figs 7 and 8, for the whole redshift range $0.1 < z < 1.5$ but also split into low ($0.1 < z < 0.8$) and high ($0.8 < z < 1.5$) redshift. In both colour–magnitude and colour–colour diagrams, the peak of the expected distribution lies at $U - V \sim 1.1$, indicating that the region where we would expect the highest number of AGN/SB hybrid sources to exist by chance is at green $U - V$ colours.

Note that up to now we have not taken into account the redshift information when computing $N_{\rm exp}$. As seen in Fig. 4, IR galaxies peak at lower redshifts than type II AGN hosts and the optically selected population in the M_V range of interest. To investigate whether the differences in the redshift distributions have an impact on $N_{\rm exp}$, we repeat the above process, this time also binning in redshift – i.e. bin i

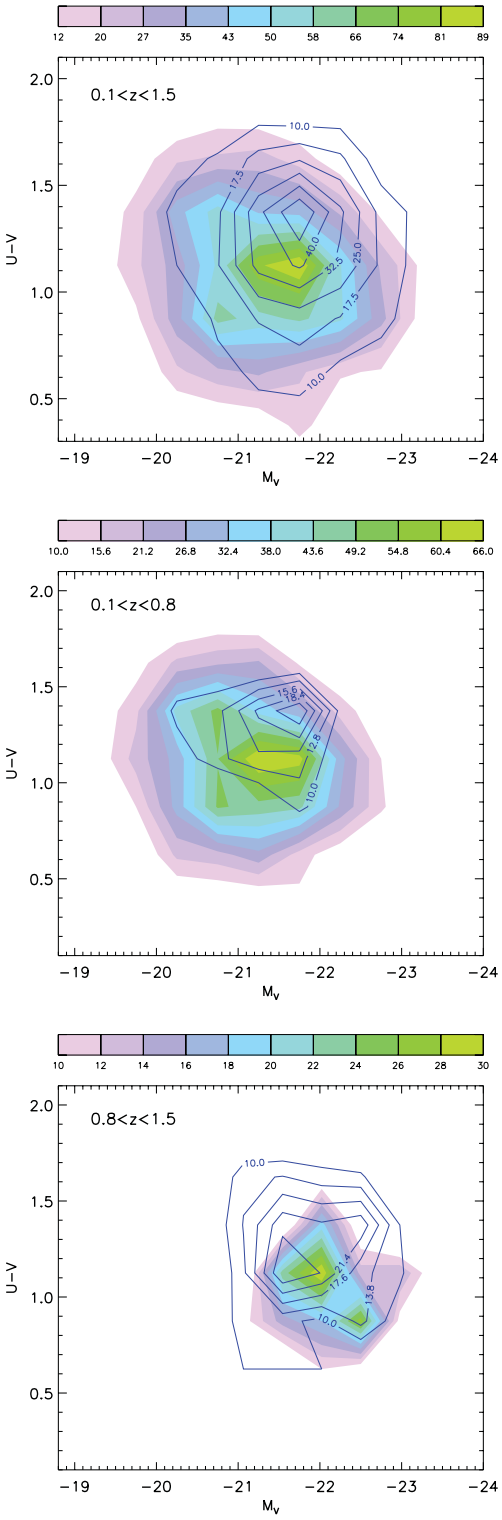

Figure 5. Rest-frame $U - V$ versus M_V for the IR galaxy sample (filled contours) and AGN host galaxies (open blue contours); the three panels correspond to different redshift ranges. The bins are 0.5 and 0.25 in size in the x and y directions, respectively, and the contours represent the number of objects. 5 contour levels are drawn for the AGN and 10 contour levels for the IR galaxies (see the colour bar), starting from n number of objects, where n is either $0.01\,N$ (where N is the total number of sources) or 10, whichever is greater.

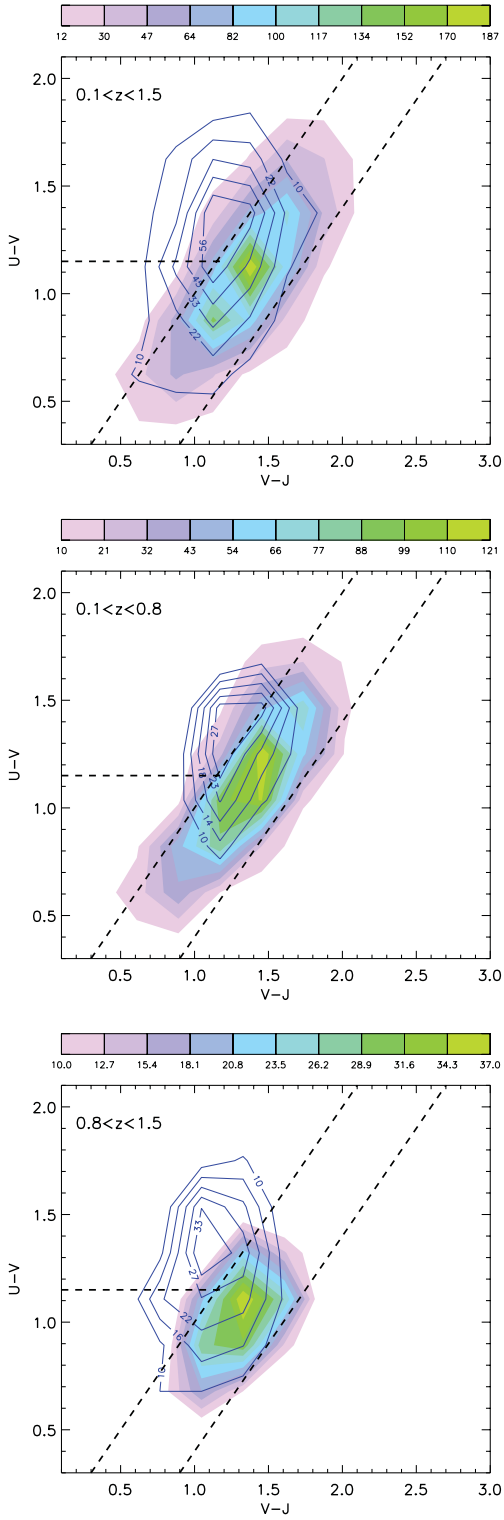

Figure 6. Rest-frame $U - V$ versus $V - J$ for the IR galaxy sample (filled contours) and AGN host galaxies (open blue contours); the three panels correspond to different redshift ranges. The dashed lines are the same as in Fig. 1. The bins are 0.25 in both axes and the contours represent the number of objects. 5 contour levels are drawn for the AGN and 10 contour levels for the IR galaxies (see the colour bar), starting from n number of objects, where n is either $0.01\,N$ (where N is the total number of sources) or 10, whichever is greater.

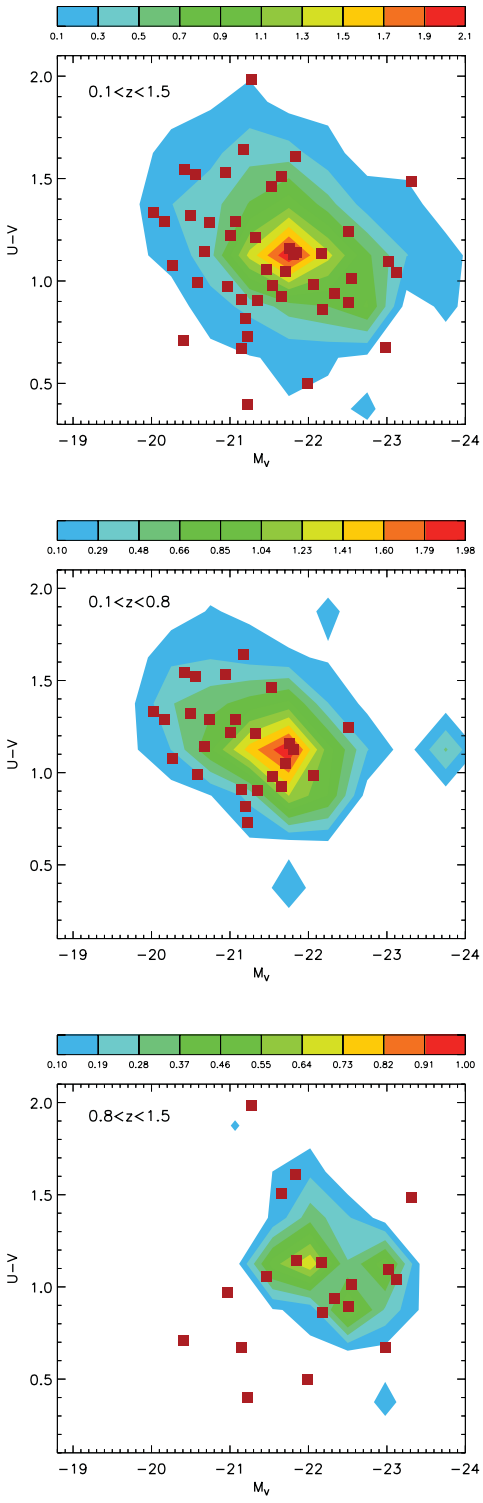

Figure 7. The colour–magnitude distribution expected for AGN/SB hybrids and computed under the assumption that AGN and star formation are independent events. The total number of expected hybrids ($N_{\rm exp} = 15.9 \pm 1$ for the top panel) is calculated by summing the number of hybrids in each bin. In all panels, the bins are 0.5 and 0.25 in size in the x and y directions, respectively, and contours correspond to the number of sources (see the colour bar). The red squares indicate the observed distribution of AGN/SB hybrids. The three panels correspond to different redshift ranges.

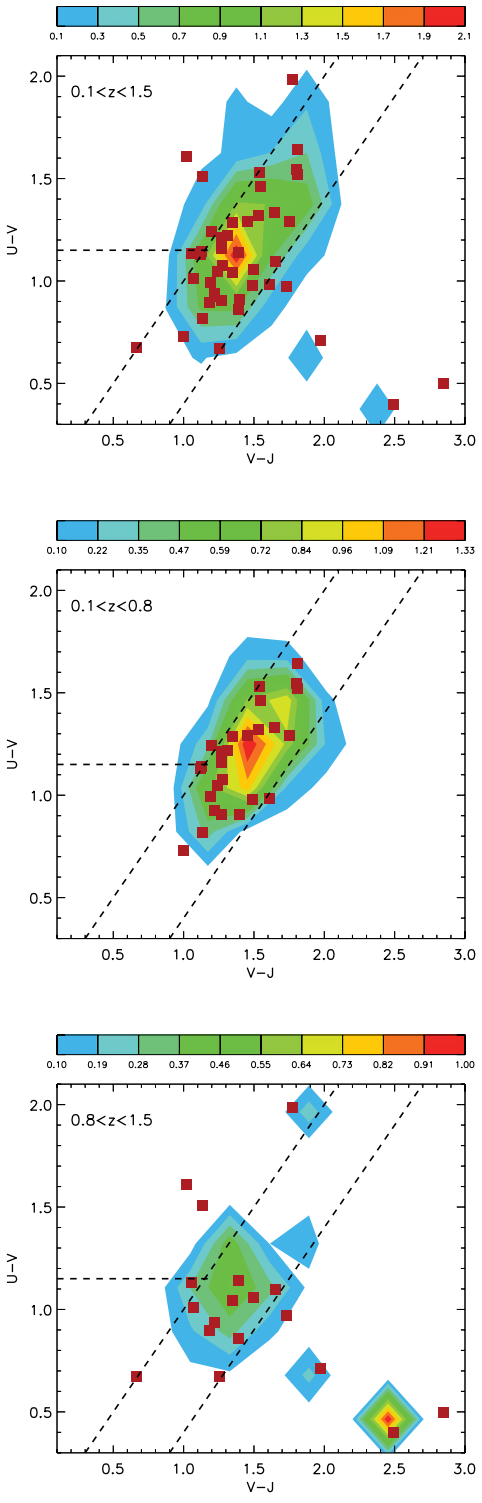

Figure 8. The colour–colour distribution expected for AGN/SB hybrids and computed under the assumption that AGN and star formation are independent events. The total number of expected hybrids ($N_{\rm exp} = 12 \pm 0.8$ for the top panel) is calculated by summing the number of hybrids in each bin. In all panels, the bins are 0.25 and 0.25 in size in the x and y directions, respectively, and contours correspond to the number of sources (see the colour bar). The red squares indicate the observed distribution of AGN/SB hybrids. The three panels correspond to different redshift ranges.

Table 1. The results of our experiment which compared the observed number of AGN/SB hybrids ($N_{\rm obs} = 45 \pm 6.7$) to the expected number of AGN/SB hybrids ($N_{\rm exp}$) computed by assuming that AGN and star formation are independent events in any given galaxy (see Section 3.2). In the first column, we show the redshift binning. 'None' indicates that the experiment is performed over the whole redshift range ($0.1 < z < 1.5$) and so the samples are only binned in colour and magnitude, whereas for 2 and 4 bins, the samples are also binned in redshift. The table examines whether $N_{\rm exp}$ is significantly different from $N_{\rm obs}$, separately for the colour–magnitude and colour–colour parameter space. $N_{\rm exp}$ (columns 2 and 5) is between two and four times lower than $N_{\rm obs}$, indicating that type II AGN are on average three times more likely to reside in dusty SFGs than would be expected serendipitously. Our calculations show that this result is significant at least at the 3σ level and on average at the 4σ level (columns 4 and 7). The significance is calculated by dividing the value of $[N_{\rm obs} - N_{\rm exp}]$ by its uncertainty (columns 3 and 6).

	Colour–magnitude			Colour–colour		
Redshift binning	$N_{\rm exp}$	$N_{\rm obs} - N_{\rm exp}$	Significance	$N_{\rm exp}$	$N_{\rm obs} - N_{\rm exp}$	Significance
None	15.9 ± 1	29.1 ± 6.8	4.3σ	12 ± 0.8	33 ± 6.8	4.9σ
2 bins	18.7 ± 1.4	26.3 ± 6.8	3.8σ	12 ± 0.9	33 ± 6.8	4.9σ
4 bins	18.6 ± 1.5	26.4 ± 6.9	3.8σ	11.6 ± 1	33.4 ± 6.8	4.9σ

is now a colour–magnitude redshift bin or a colour–colour redshift bin. We perform the experiment with two redshift bins $0.1 < z < 0.8$ and $0.8 < z < 1.5$ and subsequently with four redshift bins of equal size ($0.1 < z < 0.45$, $0.45 < z < 0.8$, $0.8 < z < 1.15$, $1.15 < z < 1.5$). The computed values of $N_{\rm exp}$ and corresponding uncertainties are shown in Table 1. We see that binning in redshift does not substantially change $N_{\rm exp}$ and it is difficult to say whether the small changes are due to the different redshift distributions or statistical fluctuations which come into play when binning (small-number statistics).

Note that $N_{\rm exp}$ is higher in colour–magnitude than colour–colour space. This is because the two diagrams illustrate different galaxy properties and it is evident that there is a larger overlap between type II AGN hosts and IR galaxies in colour–magnitude space than in colour–colour space (see the top panels of Figs 5 and 6).

We remind the reader that the observed number of hybrids ($N_{\rm obs}$) is 45 with a Poisson error of $\sqrt{45}$ (= 6.7). To examine whether the difference between $N_{\rm exp}$ and $N_{\rm obs}$ is significant, we divide $[N_{\rm obs} - N_{\rm exp}]$ by its corresponding uncertainty (see Table 1). We find that in all cases $N_{\rm exp}$ is significantly lower than $N_{\rm obs}$ by at least 3σ and on average by 4σ. The ratio of $N_{\rm obs}$ to $N_{\rm exp}$ (see Table 1) indicates that type II AGN are on average three times more likely to reside in dusty SFGs than would be expected serendipitously. Regarding the question posed earlier, our results imply that the existence of AGN hosts and IR-luminous galaxies in the same part of colour–magnitude and colour–colour space is *not* coincidental. Instead, it is likely symptomatic of a link between black hole accretion and star formation. We speculate that this is a consequence of the large reservoirs of gas (e.g. Ivison et al. 2011) or merger events (e.g. Kartaltepe et al. 2010b, 2012) that often characterize IR-luminous galaxies, creating favourable conditions both for the AGN and star formation.

Note that although we identify only a small number of AGN/SB hybrids, we are sampling a small part of the $L_{\rm IR}$–z space, as the COSMOS 70 μm survey only picks up the most IR-luminous systems at each redshift slice, i.e. we can only detect AGN hosts with high SFRs. Lowering the SFR threshold, e.g. with a deeper 70 μm survey, might allow us to detect star formation in a larger fraction of AGN hosts, in agreement with reports from other studies e.g. Brusa et al. (2009), Mainieri et al. (2011), Mullaney et al. (2012a) and Santini et al. (2012). Nevertheless, the nature of this study, which targets the most luminous systems at each redshift slice, allows us to conclude that the incidence of luminous type II AGN in strongly star forming galaxies is not a serendipitous event.

3.3 The distribution of AGN/SB hybrids in colour–magnitude and colour–colour space

We next examine whether the connection between AGN incidence and IR emission identified above also manifests as a difference between the observed and expected distributions of AGN/SB hybrids, shown in Figs 7 and 8. We perform 1D Kolmogorov–Smirnov (K–S) tests on the expected and observed distributions in $U - V$ colour and V-band magnitude (Fig. 7) and $U - V$ colour and $V - J$ colour (Fig. 8); the results are shown in Table 2. We find that the expected and observed distributions are marginally different with respect to M_V and $V - J$. Looking at Fig. 7, we note that the V-band luminosities of the AGN/SB hybrids (particularly obvious in the low-redshift bin) seem lower than expected. Similarly, Fig. 8 shows that the AGN/SB hybrids are slightly offset to bluer $V - J$ colours from the peak of the expected distribution (particularly obvious at low redshift). Although the significance of this result is marginal, it suggests that the connection between black hole accretion and star formation, established earlier, might have an imprint on the properties of a galaxy when these processes occur simultaneously. Such hybrid sources appear to have diminished optical emission relative to IR emission and bluer $V - J$ colours. If the reason for the former is higher obscuration, then one might expect redder $V - J$ colours. The fact that they are bluer in combination with lower optical luminosities perhaps suggests that the AGN/SB hybrids have lower stellar masses than expected (assuming V-band luminosity to be a proxy for stellar mass). Subsequently taking the IR luminosity as a proxy for SFR we infer that the AGN/SB hybrids (particularly those at low redshift) are characterized by higher specific SFRs. This suggests that the simultaneous black hole and stellar mass build-up in a given galaxy potentially occurs during a particularly active phase

Table 2. The significance of the K–S test performed in order to evaluate the differences in the colours and magnitudes of the observed hybrids and the expected distribution of hybrid sources (see Figs 7 and 8).

	Significance of the K–S test			
	Colour–magnitude		Colour–colour	
Redshift bin	M_V	$U - V$	$V - J$	$U - V$
$0.1 < z < 1.5$	2.5σ	1.2σ	2.4σ	1.7σ
$0.1 < z < 0.8$	2.6σ	$<1\sigma$	2.3σ	$<1\sigma$
$0.8 < z < 1.5$	1.3σ	$<1\sigma$	1.1σ	$<1\sigma$

in its star-formation history, where a large fraction of the mass is being assembled.

4 SUMMARY AND CONCLUSIONS

Type II AGN hosts and IR-luminous galaxies overlap to a large extent in colour–magnitude space at green/red $U - V$ colours ($U - V \sim 1 - 1.5$) and bright V-band magnitudes ($M_V \sim -21.5$), the latter of which is characteristic of massive galaxies. Large overlap between the populations is also seen in colour–colour ($U - V$ versus $V - J$) space, with many AGN lying within the region traditionally occupied by dusty SFGs. We find that within the region of overlap, type II AGN ($L_X > 10^{42}$ erg s^{-1}) at $z < 1.5$ are on average three times more likely (with a significance of $\sim 4\sigma$) to reside in dusty SFGs than would be expected serendipitously if black hole accretion and star formation were unrelated events. This suggests that the incidence of luminous AGN in highly star forming galaxies is not a random event; instead it indicates a link between black hole accretion and star formation, likely symptomatic of favourable conditions in these systems, such as large gas reservoirs and the ability to funnel gas towards the necessary regions, e.g. via mergers, bars, etc. Moreover, we find tentative evidence that in many sources the AGN phase is coeval with a particularly active phase in the galaxy's star-formation history, during an epoch when a large fraction of the mass is being assembled.

However, the story does not end here, as besides significant overlap, we also note some clear differences in the colour–magnitude and colour–colour distributions of AGN hosts and IR galaxies. A substantial fraction of AGN hosts are offset from the parameter space occupied by dusty galaxies, displaying bluer $V - J$ colours closer to those expected for more quiescent, post-SB galaxies. These observations suggest that type II AGN hosts are not a uniform population: some have colours indicative of star formation and dust extinction, whereas others have colours indicative of the slowing down or termination of star formation.

Although we cannot present our results as evidence of AGN feedback, we can nevertheless say that they are consistent with a scenario whereby AGN play a role in galaxy evolution. Based on our observations, we propose that massive galaxies build their black hole and stellar masses simultaneously whilst located on the dusty galaxy sequence in colour–colour space; subsequently the AGN potentially terminates star formation, but outlives this event, and thus we observe many AGN hosts in the part of colour–colour space traditionally occupied by transitional or post-SB systems.

ACKNOWLEDGEMENTS

This work is in part based on observations made with the *Spitzer Space Telescope*, which is operated by the Jet Propulsion Laboratory, California Institute of Technology under a contract with NASA and on observations obtained with *XMM–Newton*, an ESA science mission with instruments and contributions directly funded by ESA Member States and NASA.

REFERENCES

Baldry I. K., Glazebrook K., Brinkmann J., Ivezić Ž., Lupton R. H., Nichol R. C., Szalay A. S., 2004, ApJ, 600, 681
Bongiorno A. et al., 2012, MNRAS, 427, 3103
Brammer G. B. et al., 2009, ApJ, 706, L173
Brusa M. et al., 2009, A&A, 507, 1277
Brusa M. et al., 2010, ApJ, 716, 348
Capak P. et al., 2007, ApJS, 172, 99
Cappelluti N. et al., 2007, ApJS, 172, 341
Cappelluti N. et al., 2009, A&A, 497, 635
Cardamone C. N., Urry C. M., Schawinski K., Treister E., Brammer G., Gawiser E., 2010, ApJ, 721, L38
Frayer D. T. et al., 2009, AJ, 138, 1261
Georgakakis A., Nandra K., Laird E. S., Aird J., Trichas M., 2008, MNRAS, 388, 1205
Granato G. L., De Zotti G., Silva L., Bressan A., Danese L., 2004, ApJ, 600, 580
Hasinger G. et al., 2007, ApJS, 172, 29
Hickox R. C. et al., 2009, ApJ, 696, 891
Ilbert O. et al., 2009, ApJ, 690, 1236
Ivison R. J., Papadopoulos P. P., Smail I., Greve T. R., Thomson A. P., Xilouris E. M., Chapman S. C., 2011, MNRAS, 412, 1913
Kartaltepe J. S. et al., 2010a, ApJ, 709, 572
Kartaltepe J. S. et al., 2010b, ApJ, 721, 98
Kartaltepe J. S. et al., 2012, ApJ, 757, 23
Le Floc'h E. et al., 2009, ApJ, 703, 222
Lehmer B. D., Alexander D. M., Bauer F. E., Brandt W. N., Goulding A. D., Jenkins L. P., Ptak A., Roberts T. P., 2010, ApJ, 724, 559
Magorrian J. et al., 1998, AJ, 115, 2285
Mainieri V. et al., 2011, A&A, 535, A80
Martin D. C. et al., 2007, ApJS, 173, 342
Mullaney J. R., Alexander D. M., Huynh M., Goulding A. D., Frayer D., 2010, MNRAS, 401, 995
Mullaney J. R. et al., 2012, MNRAS, 419, 95
Nandra K. et al., 2007, ApJ, 660, L11
Rovilos E., Georgantopoulos I., 2007, A&A, 475, 115
Salvato M. et al., 2009, ApJ, 690, 1250
Salvato M. et al., 2011, ApJ, 742, 61
Sanders D. B. et al., 2007, ApJS, 172, 86
Santini P. et al., 2012, A&A, 540, A109
Savaglio S. et al., 2005, ApJ, 635, 260
Schawinski K., Virani S., Simmons B., Urry C. M., Treister E., Kaviraj S., Kushkuley B., 2009, ApJ, 692, L19
Scoville N. et al., 2007, ApJS, 172, 1
Shapley A. E., Steidel C. C., Adelberger K. L., Dickinson M., Giavalisco M., Pettini M., 2001, ApJ, 562, 95
Silk J., Rees M. J., 1998, A&A, 331, L1
Silverman J. D. et al., 2009, ApJ, 696, 396
Springel V., Di Matteo T., Hernquist L., 2005, MNRAS, 361, 776
Strateva I. et al., 2001, AJ, 122, 1861
Symeonidis M., Willner S. P., Rigopoulou D., Huang J.-S., Fazio G. G., Jarvis M. J., 2008, MNRAS, 385, 1015
Symeonidis M., Page M. J., Seymour N., Dwelly T., Coppin K., McHardy I., Rieke G. H., Huynh M., 2009, MNRAS, 397, 1728
Symeonidis M., Rosario D., Georgakakis A., Harker J., Laird E. S., Page M. J., Willmer C. N. A., 2010, MNRAS, 403, 1474
Symeonidis M. et al., 2011, MNRAS, 417, 2239
Treister E. et al., 2009, ApJ, 693, 1713
Weiner B. J. et al., 2005, ApJ, 620, 595
Westoby P. B., Mundell C. G., Baldry I. K., 2007, MNRAS, 382, 1541
Whitaker K. E. et al., 2011, ApJ, 735, 86
Williams R. J., Quadri R. F., Franx M., van Dokkum P., Labbé I., 2009, ApJ, 691, 1879
Wuyts S. et al., 2009, ApJ, 700, 799
Wyder T. K. et al., 2007, ApJS, 173, 293

This paper has been typeset from a TEX/LATEX file prepared by the author.